Theoretical Study of Potential Energy Surfaces for N_{12} Clusters

Qian Shu Li* and Jun Fang Zhao

The School of Chemical Engineering and Materials Science, Beijing Institute of Technology, Beijing 100081, China

Received: January 16, 2002; In Final Form: March 25, 2002

Two new isomers of N_{12} clusters were reported in addition to the four isomers previously studied. The decomposition pathways of these six N_{12} isomers were studied by using the density functional theory (DFT) method at the B3LYP/6-31G* level. Relative energies were further calculated at the B3LYP/6-311+G(3df, 2p)//B3LYP/6-31G* level. DFT predicts that the dissociation of diazobispentazole proceeds via ring breaking and the barrier height is only 4.0 kcal/mol at the B3LYP/6-311+G(3df,2p)//B3LYP/6-31G* level. The dissociation reaction of N_{12} consisting of an aromatic N_5 ring and a N_7 open chain prefers ring breaking, at a cost of 9.2 kcal/mol, to breaking a bond in the side chain. For open-chain N_{12} (C_{2h}) isomer, the B3LYP/6-311+G(3df,2p)//B3LYP/6-31G* barrier height for the N_2 elimination reaction is 14.5 kcal/mol. As for the cyclic and cagelike isomers, their decomposition barrier heights are all much lower than 10 kcal/mol. From the results presented here, it seems that these six isomers are not kinetically stable enough because of their lower barrier heights of decomposition.

Introduction

In recent years, nitrogen clusters have drawn considerable attention because of not only their theoretical interest but also their possible use as environmentally friendly high-energy−density materials (HEDMs). However, it is a challenge to synthesize the polynitrogen compounds. Indeed, for many years, the only known pure nitrogen species were molecular dinitrogen and azide ion. In 1999, Christe et al.[1] synthesized successfully a N_5^+ salt ($N_5^+AsF^-$), the third readily accessible homonuclear polynitrogen species, and received much public acclaim[2]. Recently, Christe and co-workers[3] also reported other stable fluoroantimonate salts of N_5^+. The new N_5^+ salt, $N_5^+SbF_6^-$, is surprisingly stable, decomposing only at 70 °C, and is relatively insensitive to impact. The new discovery opens a venue to neutral polynitrogen compounds and provides the basis for the first synthesis of stable nitrogen allotropes. Quite recently, Cacace et al.[4] demonstrated the existence of the tetranitrogen molecule, N_4, as a metastable species the lifetime of which exceeds 1 μs at 298 K. The identification of N_4 represents the first addition in nearly half a century to the family of the polynitrogen molecules. Hammerl and Klapötke[5] also reported a combined theoretical and experimental NMR study on nitrogen-rich compounds, tetrazolylpentazoles.

In fact, most of our understanding about polynitrogen comes from the theoretical calculations.[6−29] Previously, Glukhovtsev et al.[8] have calculated the structures and stability of neutral polynitrogen molecules (N_4, N_6, N_8, N_{10}, and N_{12}) by ab initio and density functional theory (DFT) methods. Recently, Bartlett[9] reviewed that polynitrogen compounds are elusive and potentially explosive and pointed out that quantum-chemical calculations suggest that a wealth of these compounds are just waiting to be discovered. The critical questions for all-nitrogen clusters are the barriers to dissociation and the method of synthesis. Lauderdale et al.[10] considered the molecule N_4 in a tetrahedral arrangement, as well as the N_8 analogue of cubane. In both cases, the high symmetry indicates that any decomposition to N_2 would be Woodward−Hoffmann forbidden, suggesting significant barriers to decomposition. Gagliardi et al.[11] and Nguyen et al.[12] investigated the decomposition mechanism of N_6, and a concerted transition state with C_2 symmetry has been found between the most stable diazide form of N_6 and three N_2 molecules. The computed results indicate that the neutral diazide molecule is only a short-lived species at room temperature. More recently, Bartlett et al.[13] reported that the long-sought N_6 ring can be formed by adding coordinate-covalent bonds from oxygen and these systems appear kinetically stable with a significant dissociation barrier. Schmidt et al.[14] investigated the rather complicated dissociation for the cubic N_8 and pointed out that the initial barrier is too modest to allow hope for its handling in bulk quantity. Gagliardi et al.[15,16] examined the dissociation reaction of N_8 azapentalene toward four N_2 and the stability of the bicycle N_{10} structure. Chung et al.[17] carried out the theoretical study of potential energy surfaces and the dissociation mechanisms for three low-lying energetic N_8 isomers using ab initio methods. The computed dissociation barriers of these three N_8 isomers are all less than or equal to 20 kcal/mol.

Recently, Olah et al.[24] predicted that interaction of the dications N_6^{2+} and N_4^{2+} with azide (N_3^-) ions was highly exothermic to yield N_{12} and N_{10}, respectively. On the basis of the previous theoretical studies,[8,28] four possible isomers of N_{12} have been reported. In this work, two new isomers of N_{12} were found, and to assess their stability further, the study of decomposition pathways of these six possible structures of N_{12} was also performed by a DFT method. The present study would provide some theoretical data for synthesizing more stable nitrogen clusters in the future.

Calculation Method

Calculations were carried out with the Gaussian 98 program system.[30] The geometry optimizations were performed by the

* To whom correspondence should be addressed. Fax: +86-10-6891-2665. E-mail: qsli@mh.bit.edu.cn.

10.1021/jp020110n CCC: $22.00
Published on Web 04/30/2002

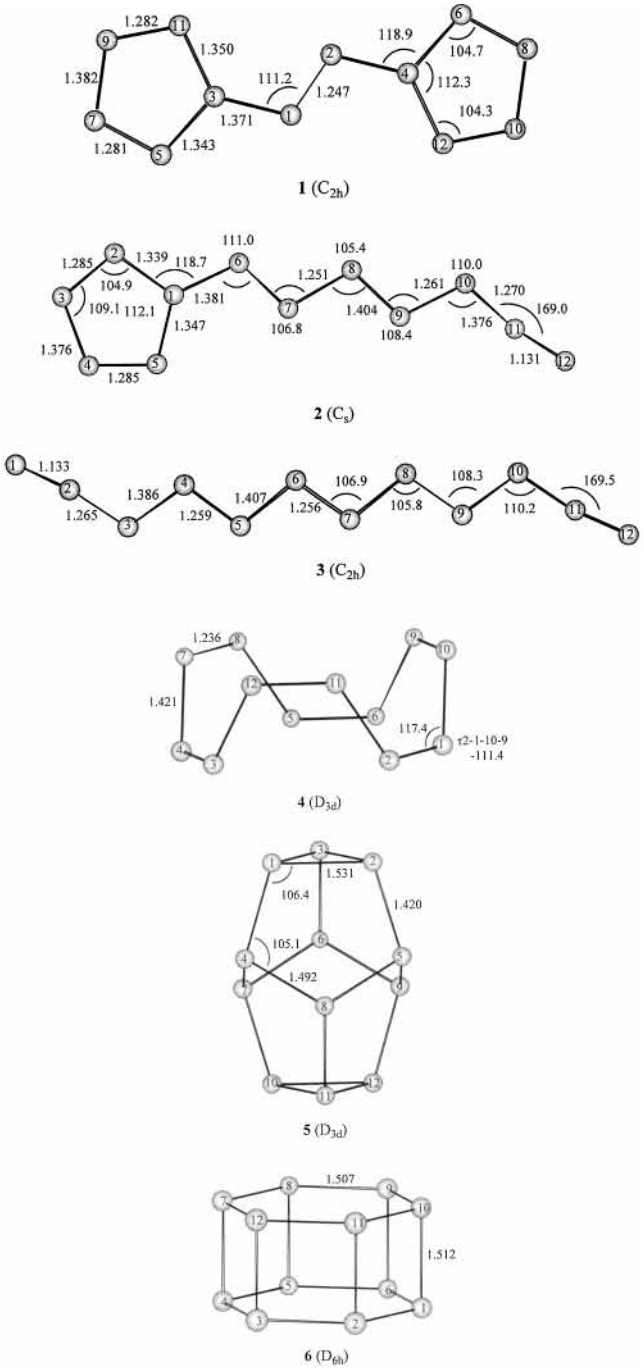

Figure 1. Optimized molecular structures for six N_{12} isomers.

density functional theory (DFT) method employing the B3LYP functional[31,32] and using the 6-31G* basis set, which is a standard split-valence double-ζ polarization basis set. Vibrational frequencies at the B3LYP/6-31G* level were used to characterize stationary points as minima (number of imaginary frequencies (NIMAG) = 0) or transition states (NIMAG = 1) and to evaluate zero-point vibrational energies (ZPE). Minimum energy pathways connecting the reactants and products were confirmed using the intrinsic reaction coordinate (IRC) method with the Gonzalez−Schlegel second-order algorithm.[33−34] Final energies were further calculated at the B3LYP/6-311+G(3df,2p)//B3LYP/6-31G* + ZPE(B3LYP/6-31G*) level of theory. Throughout this paper, bond lengths are given in angstroms, bond angles in degrees, total energies in hartrees, relative and zero-point vibrational energies, unless otherwise stated, in kcal/mol.

TABLE 1: Total Energies [*E* (hartree)], Zero-Point Energy [ZPE (kcal/mol)], and Lowest Vibrational Freqency [ν_1 (cm^{-1})] for Six N_{12} Molecules

	B3LYP/6-31G*			B3LYP/6-311+G(3df,2p)//
isomers	*E*	ZPE	ν_1	B3LYP/6-31G*
1 (C_{2h})	−656.705 628 8	35.3	37	−656.919 462 9
2 (C_S)	−656.681 526 8	33.9	38	−656.909 090 5
3 (C_{2h})	−656.650 362 4	32.3	20	−656.885 994 3
4 (D_{3d})	−656.588 910 1	31.6	126	−656.809 322 9
5 (D_{3d})	−656.387 336 6	32.8	294	−656.599 974 5
6 (D_{6h})	−656.154 051 3	31.2	208	−656.367 425 3

TABLE 2: Energy Differences (kcal/mol) Relative to Six N_2 Molecules at The B3LYP/6-311+G(3df,2p)[a]//B3LYP/6-31G* Level

$6N_2$	**1**	**2**	**3**	**4**	**5**	**6**
0.0	316.4	321.5	334.4	381.8	514.4	658.7

[a] Single-point energy in B3LYP/6-311+G(3df,2p)//B3LYP/6-31G* with ZPE correction in B3LYP/6-31G*.

Results and Discussion

1. Minimum Energy Structures. The molecular structures for six N_{12} isomers are illustrated in Figure 1, along with their computed geometrical parameters. The total energies, zero-point energies (ZPE), and lowest vibrational frequencies are summarized in Table 1. As is seen, these six N_{12} isomers are local minima on the B3LYP/6-31G* potential energy surfaces with all real vibrational frequencies.

Glukhovtsev et al.[8] has reported that isomers **1** and **3** are two energetically low-lying structures of N_{12} clusters. In 1997, we[28] studied two cagelike single-bond N_{12} isomers, **5** and **6**, and found that they are reasonable minima on the potential energy surface. Isomers **2** and **4** are two new structures reported for the first time. From Table 2, the stability ordering of the six isomers is **1** > **2** > **3** > **4** > **5** > **6**. Previous studies[8,29] have suggested that the aromatic pentazole ring is a stable structural unit for some larger even-numbered nitrogen clusters. Azidopentazole (C_S) with a five-membered ring and an open N_3 chain and bispentazole (D_{2d}) with two perpendicular five-membered rings are the minimum-energy structures among all of the known N_8 and N_{10} isomers, respectively. For the N_{12} clusters, diazobispentazole (isomer **1**) contains two aromatic pentazole rings linked by a diazo −N═N− bridge bond; therefore, it is the most stable species among these six isomers. The geometry for **2** with one aromatic N_5 ring is similar to that of the azidopentazole N_8. It is the second most stable isomer and only 5.1 kcal/mol less stable than **1** at the B3LYP/6-311+G(3df,2p)//B3LYP/6-31G* level including the zero-point energy correction. C_{2h}-symmetric open-chain structure **3** lies above **1** by 18.0 kcal/mol at the B3LYP/6-311+G(3df,2p) level. Isomer **4** is a D_{3d} symmetric cyclic molecule (Figure 1), which is about 65.4 kcal/mol less stable than isomer **1** at the above level of theory. Isomers **5** and **6** are two highly symmetric cagelike molecules and found to be high-lying in energy compared with the other four isomers discussed above. Isomer **5** and **6** lie 198.0 and 342.3 kcal/mol, respectively, above the most stable **1** at the B3LYP/6-311+G(3df,2p) level of theory. Obviously, the existence of ring strains from 60° to 90° angles decrease the stability of **5** and **6** relative to the other four isomers. On the other hand, just as considered by Ha et al.[18] for cage-form N_{20}, the nitrogen lone-pairs interaction also is a reason for the high energy of cagelike structures. The relative stability is also reflected by the geometrical parameters. The cage forms consist of weak and purely single-bonded N atoms, whereas the other isomers consist of alternatively single and double bonds.

TABLE 3: Total Energies [*E* (hartree)], Zero-Point Energy [ZPE (kcal/mol)], and Lowest Vibrational Frequency [ν_1 (cm^{-1})] for the Transition States and Products (N_{10}, N_8, and N_6 Molecules)

	B3LYP/6-31G*			B3LYP/6-311+G(3df,2p)//
isomers	*E*	ZPE	ν_1	B3LYP/6-31G*
TS1 (C_S)	−656.689 291 2	33.2	494i	−656.909 734 7
TS2 (C_S)	−656.658 338 7	32.1	721i	−656.884 975 8
TS3 (C_S)	−656.662 603 9	31.7	498i	−656.890 858 5
TS4 (C_S)	−656.625 150 4	30.5	265i	−656.860 039 8
TS5 (C_{2h})	−656.617 343 7	28.7	744i	−656.852 382 5
TS6 (C_S)	−547.219 055	26.6	711i	−547.407 189
TS7 (C_S)	−547.223 854 2	26.0	504i	−547.413 373 1
TS8 (C_S)	−547.188 496 6	24.8	747i	−547.384 476 8
TS9 (C_1)	−656.585 966 8	29.8	442i	−656.806 363 7
TS10 (C_1)	−656.381 568 1	31.2	415i	−656.593 441
TS11 (C_{2h})	−656.153 734 3	30.3	351i	−656.366 854 5
N_{10} (C_S)	−547.245 959 8	28.4	45	−547.434 982 1
N_{10} (C_{2h})	−547.216 140 6	26.8	38	−547.413 219 5
N_8 (C_S)	−437.798 565 5	22.8	42	−437.949 595 8
N_8 (C_{2h})	−437.777 754 3	21.2	66	−437.935 993 7
N_8 (D_{2h})	−437.776 399 7	23.6	246	−437.924 156 2
N_6 (C_{2h})	−328.324 645	15.3	62	−328.443 994 1

The energy of the N_2 molecule is −109.566 810 7 au at the B3LYP/6-311+G(3df,2p) level of theory. The energy differences relative to six N_2 molecules are listed in Table 2, and it appears that these six N_{12} isomers would be very energetic materials.

2. Transition Structures and Reaction Barriers for Decomposition Reaction. The N_{12} isomers might dissociate either by direct elimination of one or more N_2 molecules or by an intermediate N_{12} structure (another isomer). In our present study, the decomposition mechanisms of the six N_{12} isomers were investigated using a DFT method at the B3LYP/6-31G* level. The optimized geometric parameters for transition states (**TS1**−**TS11**) and products involving the N_{10} (C_S) molecule, open-chain N_{10} (C_{2h}) molecule, azidopentazole (C_S), and octaazapentalene (D_{2h}), as well as open-chain N_8 (C_{2h}) and N_6 (C_{2h}), are illustrated in Figure 2. Their total energies, zero-point energy (ZPE), and lowest vibrational frequency are listed in Table 3. The energy differences between the minima (isomers **1**, **2**, **3**, **4**, **5**, **6**, and two N_{10} minima) and their corresponding transition states are summarized in Table 4. The schematic potential energy surfaces for decomposition of N_{12} isomers are depicted in Figure 3. The C_{2h} symmetric open-chain N_{10}, azidopentazole, octaazapentalene, and N_8, as well as N_6, have been reported previously.[8] However, the C_S symmetric N_{10} molecule is a new isomer containing one aromatic N_5 ring and an exocyclic pentaazo (N_5) group. It is a true local minimum on the N_{10} potential energy surface with all real vibrational frequencies at the B3LYP/6-31G* level of theory.

a. Decomposition Process ***1*** *(C_{2h})* → ***TS1*** → *N_{10} (C_S) + N_2.* As discussed above, isomer **1** was identified to be the most stable form of N_{12}. It is clear that the possible N_2 elimination mechanisms of isomer **1** should include two channels: the ring breaking and the ring opening. We were unable to locate the transition state for the ring opening, but the B3LYP/6-31G* saddle-point search found a transition state (**TS1**) corresponding to direct N_2 elimination from **1**. **TS1** has C_S symmetry at the B3LYP level, but C_1 symmetry was reported by Klapötke[35] at the MP2 level. As shown in Figure 2, the bond lengths of N4−N12 and N8−N10 in **TS1** increase to 1.685 and 1.676 Å, respectively. The longer bond distances imply that the charge attraction forces between N4 and N12 and between N8 and N10 are weak and, therefore, the two bonds would break and **1** would dissociate into N_{10} (C_S) + N_2. IRC calculation performed at the same level of theory verifies that the pathway is a decomposition channel of **1**. **TS1** lies 8.2 kcal/mol above **1** at the B3LYP/6-31G* level including the zero-point energy correction, and B3LYP/6-311+G(3df,2p) single-point calculation gives a value of 4.0 kcal/mol. Such a small value suggests that it may be possible to observe this isomer only as a short-lived species, rather than one that is suitable for preparation and handling in bulk quantities.

TABLE 4: Energy Differences (kcal/mol) of Transition States Relative to Isomers 1, 2, 3, 4, 5, and 6 with ZPE Correction

isomers	B3LYP/6-31G*	B3LYP/6-311+G(3df,2p)[a]// B3LYP/6-31G*
1 (C_{2h})	0.0	0.0
TS1	8.2	4.0
2 (C_S)	0.0	0.0
TS2	12.8	13.3
TS3	9.7	9.2
3 (C_{2h})	0.0	0.0
TS4	14.0	14.5
TS5	17.1	17.5
4 (D_{3d})	0.0	0.0
TS9	0.05	0.06
5 (D_{3d})	0.0	0.0
TS10	2.0	2.5
6 (D_{6h})	0.0	0.0
TS11	−0.7	−0.5
N_{10} (C_S)	0.0	0.0
TS6	15.1	15.6
TS7	11.5	11.2
N_{10} (C_{2h})	17.1	12.1
TS8	32.5	28.1

[a] Single-point energy in B3LYP/6-311+G(3df,2p)//B3LYP/6-31G* with ZPE correction in B3LYP/6-31G*.

b. Decomposition Processes ***2*** *(C_S)* → ***TS2*** → *N_{10} (C_S) + N_2 and* ***2*** *(C_S)* → ***TS3*** → *N_{10} (C_{2h}) + N_2.* We have found two transition states for the N_2 elimination process in isomer **2**. **TS2** corresponding to side-chain breaking and **TS3** corresponding to ring breaking lie 12.8 and 9.7 kcal/mol, respectively, above **2** at the B3LYP/6-31G* level including the zero-point energy correction. The corresponding B3LYP/6-311+G(3df,2p) results are 13.3 and 9.2 kcal/mol, respectively. As can be seen in Figure 2, in **TS2**, the N11−N12 bond is 0.014 Å shorter and the breaking N10−N11 bond is elongated by about 0.3 Å compared to that in **2**. In **TS3**, the N3−N4 and N1−N5 bond lengths increase to 1.693 and 1.697 Å, respectively, while the other bond lengths and bond angles change slightly. The IRC calculation confirms that **TS2** is connected to **2** on the reactant side and to N_{10} (C_S) and N_2 on the product side. On the other hand, starting from **TS3**, the IRC leads to linear structure N_{10} (C_{2h}) and N_2, which are formed by two bonds (N1−N5 and N3−N4) breaking.

Similar trends were found in the process of N_{10} (C_S) → **TS6** → N_8 (C_S) + N_2 and N_{10} (C_S) → **TS7** → N_8 (C_{2h}) + N_2. Two transition states (**TS6** and **TS7**) are located and characterized by only one imaginary frequency at the B3LYP/6-31G* level. **TS6** corresponding to side-chain breaking and **TS7** corresponding to ring breaking lie 15.1 and 11.5 kcal/mol, respectively, above N_{10} (C_S) at the B3LYP/6-31G* level. The B3LYP/6-311+G(3df,2p) results are 15.6 and 11.2 kcal/mol, respectively. During the dissociation process from N_{10} (C_S) through **TS6** to N_8 (C_S), the bond of N8−N9, shown in Figure

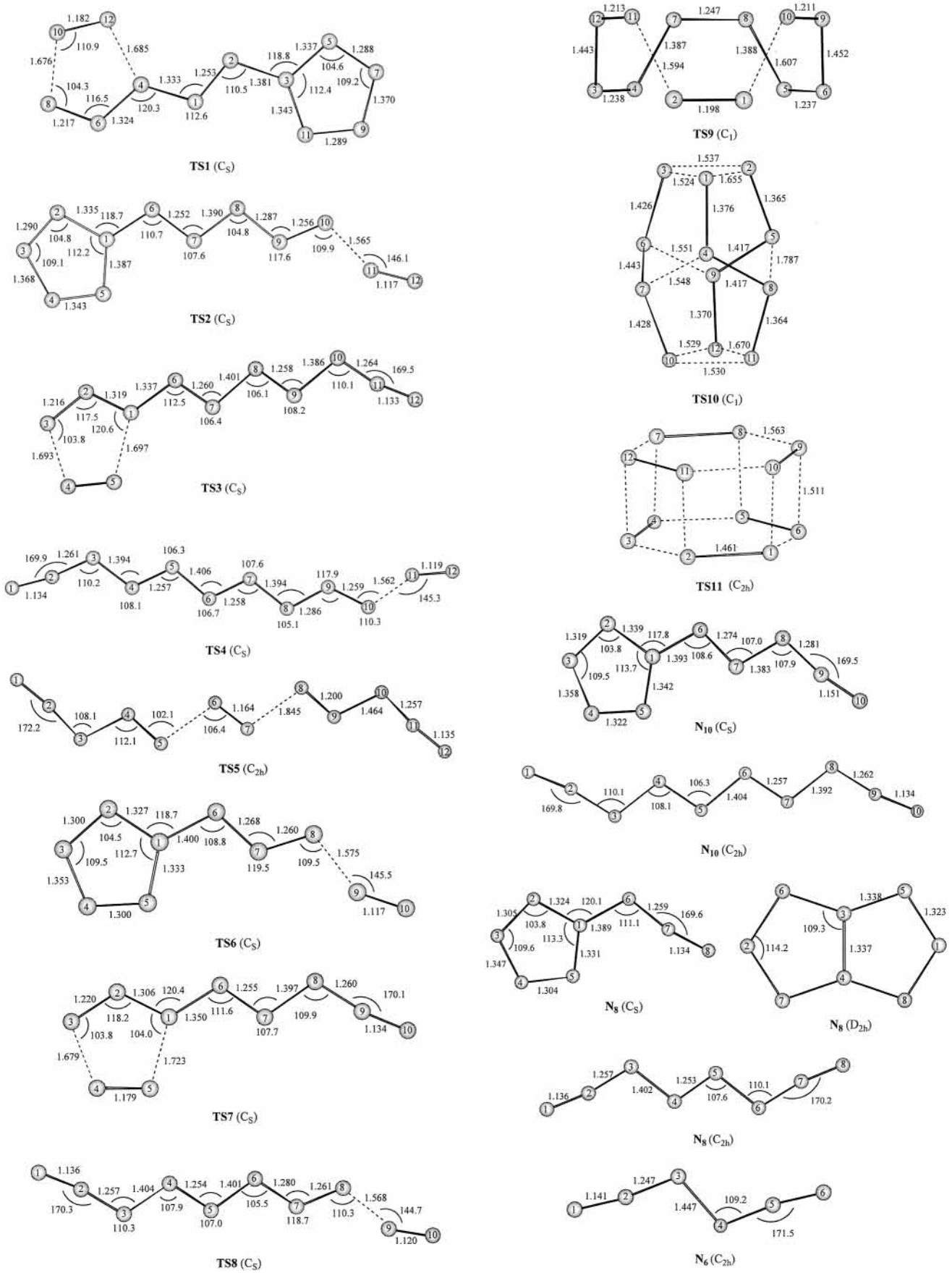

Figure 2. Transition state and involved product structures for dissociation reactions of N_{12} isomers.

2, increases by about 0.3 Å and the terminal N9−N10 bond decreases by about 0.04 Å. It is obvious that the bond of N8−N9 would break and N_{10} (C_S) would dissociate into two species: N_8 (C_S) and N_2. However, starting from **TS7**, IRC calculation performed at the B3LYP/6-31G* level leads to linear structure N_8 (C_{2h}) and N_2 molecule.

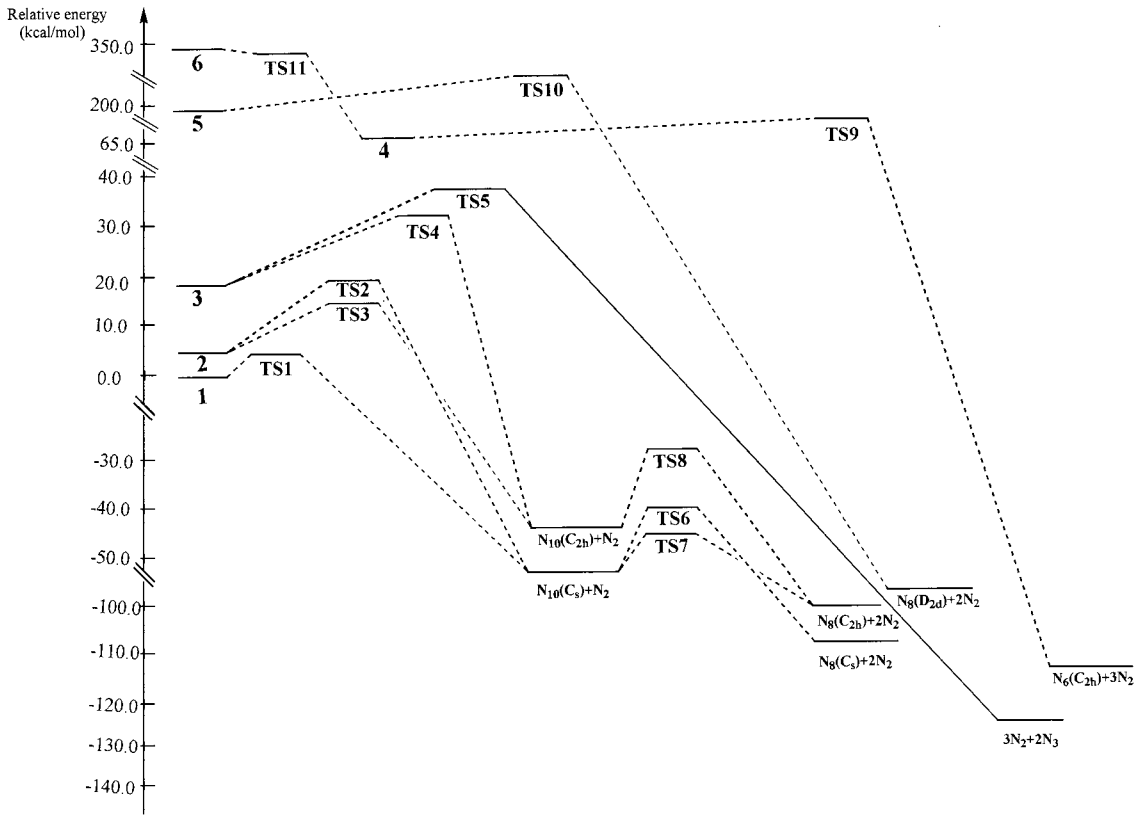

Figure 3. The schematic potential energy surfaces for dissociation reactions of N_{12} isomers.

For linear molecule N_{10} (C_{2h}), we have found a transition state, **TS8**, corresponding to direct elimination of one N_2 molecule. The calculated barrier heights are about 15.4 and 16.0 kcal/mol at B3LYP/6-31G* and B3LYP/6-311+G(3df,2p) level, respectively, including the zero-point energy correction. It was shown in the previous paper[17] that dissociation from N_8 (C_S) and N_8 (C_{2h}) to $N_6 + N_2$ proceeds with lower barriers. Therefore, isomer **2** does not appear to be a useful high-energy species.

c. Decomposition Process ***3*** *(*C_{2h}*)* → ***TS4*** → N_{10} *(*C_{2h}*)* + N_2 *and* ***3*** *(*C_{2h}*)* → ***TS5*** → $3N_2 + 2N_3$. We have located two transition structures, **TS4** and **TS5** (Figure 2), for the N_2 elimination process in structure **3**, which lie 14.5 and 17.5 kcal/mol, respectively, above **3** at the B3LYP/6-311+G(3df,2p)//B3LYP/6-31G* levels. Compared with the stable structure **3**, in **TS4**, the terminal N10−N11 lengthens by about 0.3 Å. In **TS5**, however, the central N5−N6 and N7−N8 lengthen by about 0.45 Å simultaneously with the symmetry unchanged. The IRC performed at the B3LYP/6-31G* from **TS4** leads to linear structure N_{10} (C_{2h}) and N_2 molecule. On the other hand, starting from **TS5**, the IRC calculation directly leads to dissociation into three N_2 and two N_3 fragments. The simultaneous bond breaking is presumably due to an instability of the linear N_5 radical, causing its dissociation into N_2 and N_3. Unfortunately, we were unable to locate a transition state for dissociation into two equivalents of N_6.

d. Decomposition Process ***4*** *(*D_{3d}*)* → ***TS9*** → N_6 *(*C_{2h}*)* + $3N_2$. The dissociation of the cyclic isomer **4** was investigated at the B3LYP/6-31G* level of theory. A transition state (**TS9**, Figure 2) with one imaginary frequency (442i) was found only lying 0.06 kcal/mol above **4** at the B3LYP/6-311+G(3df,2p) level. IRC calculation performed at the B3LYP/6-31G* leads to a linear N_6 and three N_2 fragments. The N1−N10, N2−N11, N3−N12, and N6−N9 bonds break simultaneously to produce these products. However, the very low barrier height of decomposition for **4** suggests cyclic N_{12} cannot exist as a discrete species.

e. Decomposition Process of Cagelike Isomers ***5*** *and* ***6****:* ***5*** *(*D_{3d}*)* → ***TS10*** → N_8 *(*D_{2h}*)* + $2N_2$ *and* ***6*** *(*D_{6h}*)* → ***TS11*** → ***4*** *(*D_{3d}*)* → ***TS9*** → N_6 *(*C_{2h}*)* + $3N_2$. From the structural point, we think that the cagelike isomers consisting of five-membered rings, three-membered rings, and six-membered rings should be unstable with respect to decomposition into multiple fragments. **TS10** is found and characterized by only one imaginary frequency (415i) at the B3LYP/6-31G* level. At our B3LYP/6-311+G(3df,2p) level, **TS10** is only 2.5 kcal/mol higher in energy than **5**. Starting from **TS10**, IRC calculation leads to the formation of the D_{2h} symmetric N_8 species and two N_2 molecules.

DFT calculation suggests that the dissociation of **6** proceeds via an isomerization. Indeed, a transition state, **TS11**, has been found that connects two minima, **6** and **4**, on the potential energy surface. We should note that **TS11** is only 0.2 kcal/mol higher in energy than **6** at the B3LYP/6-31G* level without ZPE correction. When ZPE are included and at higher level of theory, **TS11** is lower in energy than **6**, as shown in Table 2. Therefore, **6** cannot exist as a discrete species, and we did not discuss it further.

Summary

The present DFT study at the B3LYP/6-31G* level shows two new isomers (**2** and **4**) are local minima on potential energy surfaces of N_{12}. Isomer **2** consisting of an aromatic N_5 ring and an open N_7 side chain is only 5.1 kcal/mol less stable than **1** (diazobispentazole) at the B3LYP/6-311+G(3df,2p)//B3LYP/6-31G* level of theory. The mechanisms for the dissociation of six isomers, including the four isomers previously studied, have also been investigated with the DFT method. It is suggested that the dissociation pathway of **1** proceeds via a ring breaking and the barrier height of the process **1** → N_{10} (C_S) + N_2 is 4.0 kcal/mol at the B3LYP/6-311+G(3df,2p)//B3LYP/6-31G* level

of theory. The dissociation reaction of **2** prefers ring breaking, at a cost of less than 20 kcal/mol, to breaking a bond in the side chain. For open-chain structure **3**, the B3LYP/6-311+G-(3df,2p)//B3LYP/6-31G* barrier height for N_2 elimination is about 14.5 kcal/mol. As for D_{3d}-symmetric cyclic isomer **4**, as well as two cagelike isomers **5** and **6**, their decomposition barrier heights are all much lower than 10 kcal/mol. From the results presented here, it seems that these six isomers are not stable enough to be high-energy−density molecules because of their lower barrier heights of decomposition.

References and Notes

(1) Christe, K. O.; Wilson, W. W.; Sheehy, J. A.; Boatz, J. A. *Angew. Chem., Int. Ed.* **1999**, *38*, 2004.
(2) See, for example: *Chem. Eng. News* **1999**, *77* (Jan 25), 7; **1999**, *77* (Nov 29), 38; **2000**, *78* (Aug 14), 41.
(3) Vij, A.; Wilson, W. W.; Vij, V.; Tham, F. S.; Sheehy, J. A.; Christe, K. O. *J. Am. Chem. Soc.* **2001**, *123*, 6308.
(4) Cacace, F.; Petris, G.; Troiani, A. *Science* **2002**, *295*, 480.
(5) Hammerl, A.; Klapötke, T. M. *Inorg. Chem.* **2002**, *41*, 906.
(6) Pykkö, P.; Runeberg, N. *J. Mol. Struct.* (*THEOCHEM*) **1991**, *234*, 279.
(7) Lee, T. J.; Rice, J. E. *J. Chem. Phys.* **1991**, *94*, 1215.
(8) Glukhovtsev, M. N.; Jiao, H.; Schleyer, P. v. R. *Inorg. Chem.* **1996**, *35*, 7124.
(9) Bartlett, R. J. *Chem. Ind*. **2000**, *4*, 140.
(10) Lauderdale, W. J.; Stanton, R. F.; Bartlett, R. J. *J. Phys. Chem.* **1992**, *96*, 1173.
(11) Gagliardi, L.; Evangelisti, S.; Barone, V.; Roos, B. O. *Chem. Phys. Lett.* **2000**, *320*, 518.
(12) Nguyen, M. T.; Ha, T.-K. *Chem. Phys. Lett*. **2001**, *335*, 311.
(13) Wilson, K. J.; Perera, S. A.; Bartlett, R. J. *J. Phys. Chem. A* **2001**, *105*, 7693.
(14) Schmidt, M. W.; Gordon, M. S.; Boatz, J. A. *Int. J. Quantum Chem.* **2000**, *76*, 434.
(15) Gagliardi, L.; Evangelisti, S.; Bernhardsson, A.; Lindh, R.; Roos, B. O. *Int. J. Quantum Chem.* **2000**, *77*, 311.
(16) Gagliardi, L.; Orlandi, G.; Evangelisti, S.; Roos, B. O. *J. Chem. Phys*. **2001**, *114*, 10733.
(17) Chung, G.; Schmidt, M. W.; Gordon, M. S. *J. Phys. Chem.* A **2000**, *104*, 5647.
(18) Ha, T.-K.; Suleimenov, O.; Nguyen, M. T. *Chem. Phys. Lett*. **1999**, *315*, 327.
(19) Korkin, A.; Balkova, A.; Bartlett, R. J.; Boyd, R. J.; Schleyer, P. v. R. *J. Phys. Chem.* **1996**, *100*, 5702.
(20) Dunn, K.; Morokuma, K. *J. Chem. Phys*. **1995**, *102*, 4904.
(21) Tobita, M.; Bartlett, R. J. *J. Phys. Chem*. **2001**, *105*, 4107.
(22) Gimarc, B. M.; Zhao, M. *Inorg. Chem.* **1996**, *35*, 3289.
(23) Xin, W.; Hu, H−R.; Tian, An-M.; Wong, N. B.; Chien, Siu-H.; Li, W.-K. *Chem. Phys. Lett.* **2000**, *329*, 483.
(24) Olah, G. A.; Prakash, G. K. S.; Rasul, G. *J. Am. Chem. Soc.* **2001**, *123*, 3308.
(25) Bliznyuk, A. A.; Shen, M.; Schaefer, H. F. *Chem. Phys. Lett*. **1992**, *198*, 249.
(26) Tian, An-M.; Ding, F.-J.; Zhang, L.-F.; Xie, Y.-M.; Schaefer, H. F. *J. Phys. Chem. A* **1997**, *101*, 1946.
(27) Li, Q.-Shu.; Wang, L.-J. *J. Phys. Chem. A* **2001**, *105*, 1979.
(28) Qu, H.; Li, Q.-Shu.; Zhu, H.-Sun. *Chin. Sci. Bull.* **1997**, *42*, 462.
(29) Manaa, M. R. *Chem. Phys. Lett*. **2000**, *331*, 262.
(30) Frisch, M. J.; Trucks, G. W.; Schlegel, H. B.; Scuseria, G. E.; Robb, M. A.; Cheeseman, J. R.; Zakrzewski, V. G.; Montgomery, J. A., Jr.; Stratmann, R. E.; Burant, J. C.; Dapprich, S.; Millam, J. M.; Daniels, A. D.; Kudin, K. N.; Strain, M. C.; Farkas, O.; Tomasi, J.; Barone, V.; Cossi, M.; Cammi, R.; Mennucci, B.; Pomelli, C.; Adamo, C.; Clifford, S.; Ochterski, J.; Petersson, G. A.; Ayala, P. Y.; Cui, Q.; Morokuma, K.; Malick, D. K.; Rabuck, A. D.; Raghavachari, K.; Foresman, J. B.; Cioslowski, J.; Ortiz, J. V.; Stefanov, B. B.; Liu, G.; Liashenko, A.; Piskorz, P.; Komaromi, I.; Gomperts, R.; Martin, R. L.; Fox, D. J.; Keith, T.; Al-Laham, M. A.; Peng, C. Y.; Nanayakkara, A.; Gonzalez, C.; Challacombe, M.; Gill, P. M. W.; Johnson, B. G.; Chen, W.; Wong, M. W.; Andres, J. L.; Head-Gordon, M.; Replogle, E. S.; Pople, J. A. *Gaussian 98*, revision A.9; Gaussian, Inc.: Pittsburgh, PA, 1998.
(31) Becke, A. D. *J. Chem. Phys.* **1993**, *98*, 5648.
(32) Lee, C.; Yang, W.; Parr, R. G. *Phys. Rev.* B **1988**, *37*, 785.
(33) Gonzalez, C.; Schlegel, H. B. *J. Chem. Phys*. **1989**, *90*, 2154.
(34) Gonzalez, C.; Schlegel, H. B. *J. Phys. Chem.* **1990**, *94*, 5523.
(35) Klapötke, T. M.; Harcourt, R. D. *J. Mol. Struct.* (*THEOCHEM*) **2001**, 541, 237.